

# Wafer-scale Hierarchically Textured Silicon for Surface Cooling

Jonathan Sullivan, Laia Ferrer-Argemi, Ziqi Yu, Jaeho Lee

Department of Mechanical and Aerospace Engineering

University of California, Irvine

Irvine, CA, USA, 92617

Email: jaeholee@uci.edu

## ABSTRACT

Conventional surface materials for cooling systems, often based on metals, generally offer excellent mechanical and thermal conduction properties. However, metals are known to be very reflective, and their emissivity is very low, which limits effective radiative heat transfer from the surface to the environment – a factor that is particularly important when there is a high difference in temperature between the surface and ambient. Here we will demonstrate a novel material coating based on silicon that will offer transformative surface cooling and omniphobic properties by controlling the microscale surface texture on silicon wafers. Surface texturing silicon or micro-structuring silicon using maskless chemical assisted etching or reactive-ion etching has received much attention recently for its applications in photonics and solar cells<sup>1-3</sup>. Colloquially referred to as “black silicon”, textured silicon surfaces comprised of micro-structured pillars or roughness have been known to absorb (or emit) light very effectively in the visible spectrum, which makes the surface turn black<sup>4-6</sup>. Past studies have focused on the modified optical properties in the visible to near-infrared spectrum (400nm to 1.3um), relevant mostly to photonic applications, but we show that the optical properties maintain a high emissivity across the near-mid IR spectrum of 9-13 um. The high emissivity across the mid-IR creates a unique opportunity to produce an inexpensive, highly adaptable, and scalable layer which demonstrates enhanced passive surface cooling relative to conventional materials. We will demonstrate a novel maskless process that utilizes a NaOH wet etch which generates micro-pyramidal structures on the order of 5-20 um in height that accomplishes these objectives. Furthermore, by texturing the surface geometry, textured silicon can also be manufactured to offer either hydrophobic or hydrophilic properties, opening the possibility for a material that can have optimized conductive, radiative, and convective properties.

**KEY WORDS:** Black Silicon, Passive Cooling, Selective Emitters, Textured Silicon, Micro-pyramidal Silicon

## NOMENCLATURE

|                |   |
|----------------|---|
| P              | power per unit area (W/m <sup>2</sup> )                                 |
| h              | Planck constant (m <sup>2</sup> kg/s)                                   |
| k <sub>b</sub> | Boltzmann constant (m <sup>2</sup> kg s <sup>-2</sup> K <sup>-1</sup> ) |
| T              | temperature (K)   |
| c              | speed of light in a vacuum (m/s)  |
| t              | atmospheric transmittance   |
| IR             | infrared  |
| NIR            | Near-infrared   |
| FTIR           | Fourier Transform Infrared Spectroscopy                                 |
| h <sub>c</sub> | net heat transfer coefficient (W/m <sup>2</sup> K)                      |

## Greek symbols

|            |                                   |
|------------|-----------------------------------|
| $\lambda$  | wavelength (um)                   |
| $\epsilon$ | emissivity                        |
| $\theta$   | incident angle                    |
| $\Omega$   | angle of the hemisphere, vertical |
| $\Phi$     | angle of the hemisphere, planar   |

## Subscripts

|      |            |
|------|------------|
| atm  | atmosphere |
| conv | convection |
| cond | conduction |

## INTRODUCTION

Typical surface materials based on metal are often used due to metals’ excellent intrinsic mechanical and thermal conduction properties. However, from a radiative perspective, metals are known to be very reflective, and accordingly metallic emissivity values are very low (generally below 0.1), which limits radiative heat transfer from the surface to the environment. Instead of using a metal as a surface material, utilizing textured silicon on a surface not only maximizes the emissivity but also enables omniphobicity as well as excellent thermal conduction. Surface texturing silicon or micro-structuring silicon has received much attention for solar cells and photonic applications [1-3]. Colloquially referred to as “black silicon”, silicon surfaces comprised of micro-structured pillars or roughness have been known to absorb (or emit) light very effectively in the visible spectrum, which makes the surface optically black [4,5]. While past studies have focused on the modified optical properties in the visible to near-infrared spectra, the emissivity spectrum relevant for heat transfer is in the mid-infrared range, as governed by the Planck distribution. The concept being that a silicon surface with controlled texture will maintain a high broadband emissivity in the mid-infrared range for effective radiative cooling while also serving as an omniphobic surface. Thus, the textured silicon-based high emissivity material will create a unique opportunity to produce a relatively inexpensive, highly adaptable, and scalable layer since the silicon-based fabrication processes are very well known and established [6-12]. Our computational results demonstrate that the textured silicon is significantly more emissive than bare silicon or metals in the mid-IR, enabling substantial surface cooling without running any electricity or utilizing heat exchangers. By controlling the surface geometry, the textured silicon can also offer hydrophobic and flexible properties, which open up applications for low maintenance surface coatings that provide passive thermal control in both open-air and contained environments.

While various fabrication techniques exist for surface texturing, reactive ion-etching (RIE) and metal-assisted

etching (MAE) have been established to provide scalable approaches. As already stated, the goal is to manufacture large-scale surface textures on silicon and to increase the emissivity. The RIE and MAE methods have been used in the literature to decrease the reflectivity, which is the inverse of emissivity for opaque bodies, and achieve a low sensitivity to the angle of incidence [4]. One of the most often used methods in literature to fabricate black silicon is RIE. Using RIE, antireflection silicon surface can be prepared with a one-step and maskless process—attributes which are extremely attractive from an industrial and mass production standpoint. RIE is typically performed between the temperatures of 60 to 100°C using SF<sub>6</sub> and O<sub>2</sub> as reaction gases under optimized values of pressure, system temperature, flow rate, and radio frequency, and can be performed over a large surface area within 30-40 mins at room temperature without the need for large cooling chambers [4]. While this method is fast and scalable, it is largely indiscriminate in the micro-pillars of silicon it creates and can be very expensive as it requires highly specialized equipment and processes to fabricate. Conversely, MAE approaches yield similarly black structures at a much lower cost. Chemical etching approaches are very well known and reliable, and like RIE, also does not require a mask for the etchant. Additionally, black silicon fabricated with a chemical etchant maintains the ability to be further processed into a hierarchical structure [5], and past results demonstrate it can be more mechanically robust than RIE fabricated black silicon with the added benefit of being superhydrophobic [13-15]. The results here—and the black silicon fabricated—have been done using a MAE method. Combining both fabrication techniques, however, could enable flexible and even more adaptable silicon-based structures; this is a topic which will be discussed but has not yet been done from a fabrication standpoint. In all, we will evaluate the potential for this material from a computational standpoint, demonstrate fabrication of black silicon using a MAE process, and then discuss future outlooks and potential applications.

## RESULTS AND DISCUSSION

### Computation of Spectral Emissivity

Rigorous Coupled Wave Analysis (RCWA, 1-D) is used to calculate the surface reflectance of the textured silicon with pyramid surface structures in the wavelength range of 300 nm and 20  $\mu\text{m}$ . RCWA is a rigorous solution to Maxwell's equations which is well suited for solving for the reflection and transmission matrices of micro/nanoscale periodic optical systems. The optical constants and material properties used in the computations are from references [16-18], and it should be noted that the incident radiation is assumed to be at an angle of 30 degrees. Within RCWA, we are considering a “one-dimensional” case with an assumed infinite length along the x-axis and specified layer thickness along the y-axis. The geometry, as seen in **Fig. 1a**, is comprised of a triangle with height equal to its base made of silicon surrounded by air (**Fig. 1b**). The resultant reflectivity is shown in **Fig. 2**, and, similar to the black silicon investigated by [4,5], is extremely low

within both the visible light range(300-1200 nm) and low to mid-IR (1-20  $\mu\text{m}$ ). There is a slight (2-3%) increase in the average reflectivity in the IR-range relative to the reflectivity of nanostructured silicon in the visible spectrum, but the reflectivity is still significantly reduced relative to bulk unstructured silicon. This is especially true when compared to metals such as aluminum (**Fig. 3**) which are characteristically reflective—as denoted by the “shine” that is typically seen on the surface of a metal. For the computation of emissivity, it is assumed that the material is optically opaque as the thickness of the substrate would be enough to negate any transmission of radiation, and thus, the emissivity is computed as simply  $E = 1 - R$ .

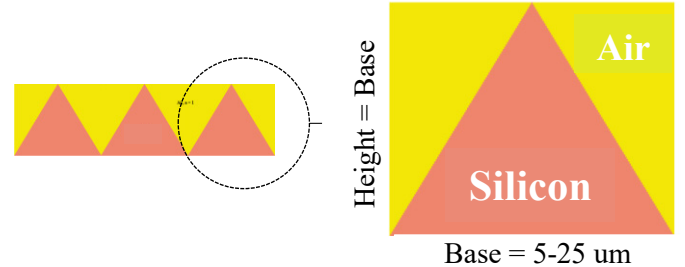


**Fig. 1** Example 2-D cross-section/unit cell being simulated within RCWA. The periodicity in this case is 25  $\mu\text{m}$ . The outer (yellow) material is optically considered air while the inner material (red) is comprised of optically homogeneous bulk silicon. A stair case approximation with many steps is used to best approximate the triangular unit cell.

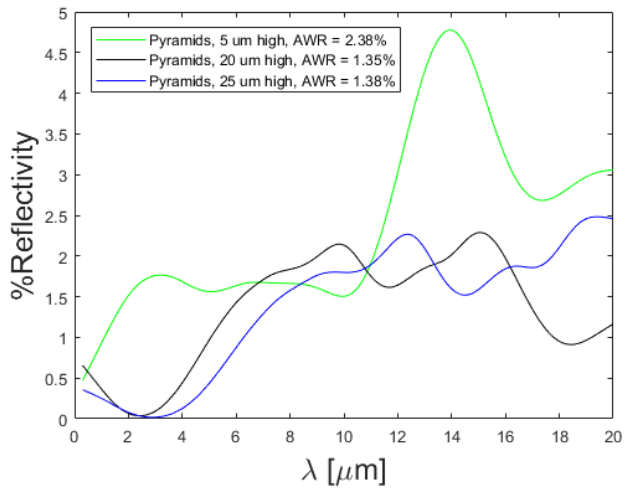


**Fig. 2** The reflectivity of the textured silicon with triangular periodicity as computed by RCWA. The base width is the same as the triangle's height; thus, the base angle is the same for all three designs. As shown in the literature [4], the average reflectivity (AR) is approximately 0.5-1% between 300-1200 nm, with slight increases in AR as the wavelength increases beyond approximately 2-3  $\mu\text{m}$ , which is promising for surface cooling, assuming no incident solar radiation.

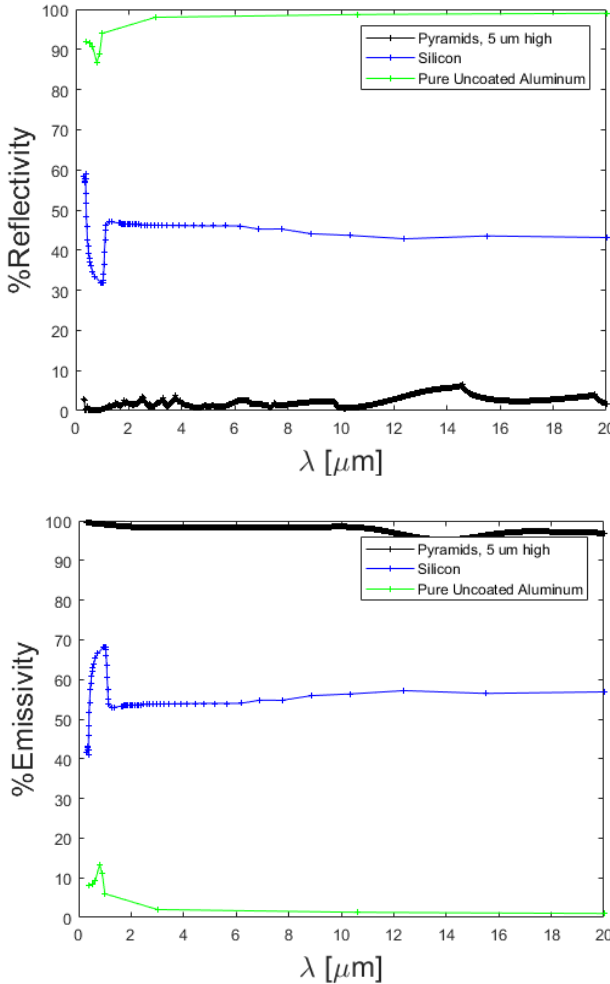


**Fig. 1 (a)** Comparison of reflectivity coefficients vs. wavelength for the triangular structure(s), bare silicon, and pure uncoated aluminum [19,20]; aluminum of this variety is often found in optical devices due to its extremely high reflectivity. With a reflectivity of approximately 0.91-0.98 (emissivity of 0.02-0.09) this surface will heat up dramatically when exposed to incident radiation, relative to the ambient temperature. **(b)** Emissivity as a function of wavelength following  $E = 1 - R$ . The emissivity of the textured silicon resembles that of a blackbody, which is the theoretical limit for radiation, promising substantial radiative cooling performance.

#### Thermal Analysis

The computation of the emissivity profile allows for immediate prediction of surface temperature with respect to the ambient for a normal day in California. The ambient temperature is 300 K (23°C, room temperature) and convective/conductive losses are assumed to be lumped into a net heat transfer coefficient of 10 W/m<sup>2</sup>K. In the case where the structure is exposed to the atmosphere, the heat balance of the structure is a function of the total incident solar irradiance, atmospheric irradiance, net radiation from the surface, and parasitic convection/conduction losses. Or,

$$-P_{\text{sun}} - P_{\text{atm}}(T_a) + P_{\text{rad}}(T) - P_{\text{conv+cond}} = P_{\text{cool}} \quad (1)$$

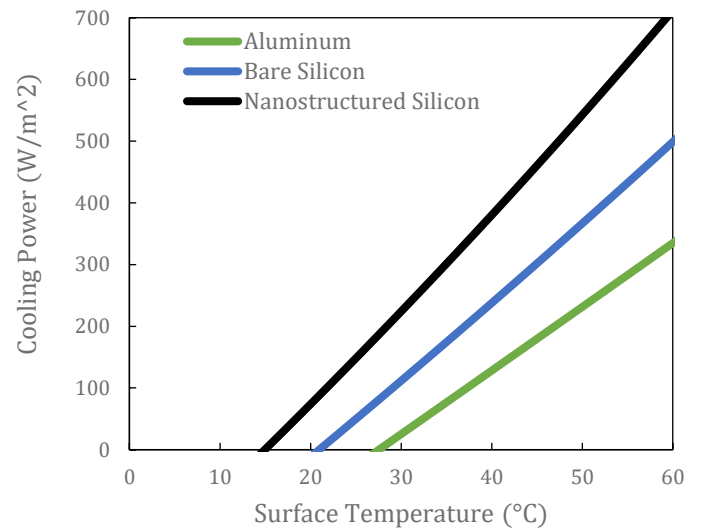
Where the radiative contributions are calculated using (simplified form) equations 2 and 3.

$$P_{\text{rad}}(T) = \int_0^{\infty} I_{\text{BB}}(T, \lambda) \epsilon(\lambda, \Omega) d\lambda \quad (2)$$

$$I_{\text{BB}}(T, \lambda) = \frac{2hc^2}{\lambda^5 \left( e^{\frac{hc}{k_b T}} - 1 \right)} \quad (3)$$

For the atmospheric contribution, an additional term is added for the emissivity of the atmosphere, which is calculated as a function of the atmospheric transmittance. The solar irradiance term, that is, the contribution of incident solar radiation, can be derived by setting  $I_{\text{BB}}$  to that of the solar irradiance for an airmass of 1.5. If a locality is preferred, as is in this case, local seasonal solar irradiance values can be used to describe the solar radiative term. Additionally, it should be noted that the emissivity is assumed to be diffuse and not dependent on temperature – reasonable assumptions considering the low range of temperature values used and past studies on the spectrally diffuse nature of black silicon [4].

The resultant analysis yields that the nanostructured silicon's surface temperature is approximately 3.6°C beneath the ambient value, in the case where there is no solar irradiance. This is a significant reduction relative to that of the silicon, which experiences a 4.2°C rise above the ambient value. The comparative cooling power for aluminum, bare silicon, and the nanostructured silicon are shown in **Fig. 4**. Clearly, the significantly reduced reflectivity is a result of the nanostructuring and has a large impact on the surface's ability to cool. We can assume that coating a surface with black silicon could enhance overall system cooling efficiency and capabilities under minimal solar irradiance. Compared to a simple black paint, this surface has the added benefit of being self-cleaning due to the omniphobic nature of the material [4,13-15]. Further, as this the radiative cooling process is completely passive, the increased cooling performance comes at no additional energy cost and requires no active components to operate or maintain.



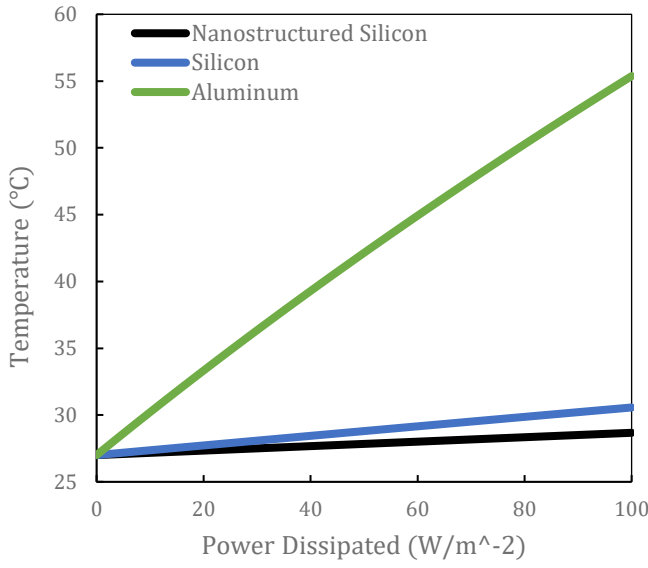


**Fig. 4.** (a) Net Radiative Cooling Power vs. the Surface Temperature, based on the emissivity information in Fig. 3a. Materials with a higher emissivity in the mid-IR (atmospheric transmission window) will effectively cool as energy is emitted from the structure into space. At a surface temperature of 50° C, the cooling powers are 106.9 W/m<sup>2</sup>, 238.2 W/m<sup>2</sup>, and 418.7 W/m<sup>2</sup> for Aluminum, Silicon, and the nanostructured or textured silicon, respectively. (b) Surface Temperature vs. an arbitrary input power in the absence of solar irradiance or atmospheric interference. Analyzed for an indoor environment with an ambient temperature of 300 K (23° C) and no convection/conduction losses, the nanostructured or textured silicon rises only 3°C above the ambient at 100 W/m<sup>2</sup>, compared to the 32°C rise experienced by aluminum at the same heat flux. Surface temperature in this case is computed using the simple Stephen Boltzmann equation,  $P = \epsilon\sigma(T^4 - T_a^4)$ .

#### Fabrication

Metal-assisted chemical etching (MACE) was utilized in the fabrication of the micropyramidal silicon. The etching solution was prepared by dissolving 9 g of Na<sub>2</sub>SiO<sub>3</sub> into 18 g NaOH solution with constant stirring in a pyrex crystallizing dish. The dispersed Na<sub>2</sub>SiO<sub>3</sub> particles will serve as the nanomask during the wet etching, but it should be noted that no mask was utilized in the fabrication of the microsurface. 50 ml of isopropyl alcohol was then added into the solution together with 535 ml deionized water. The dish containing the etching solution was heated on a hotplate to 80 °C and the silicon wafer was put in. When the etching started, bubbles could be observed. The etching lasted for 20 minute and the appearance of the wafer gradually turned from polished to anti-reflective as a result of anisotropic etching of silicon in alkalic solution. Similar to other studies, this process yields a micropyramidal structure with a height 5-10 µm and a fixed angle at the base [4]; the precise topography is a function of the etching conditions. To form pyramidal textures on a 4" silicon wafer, the wafer was first cleaned by RCA-1 process. Scanning electron microscopy

images showed the formation of pyramidal structures on the silicon wafer surface (Fig.5). The geometric parameters of the

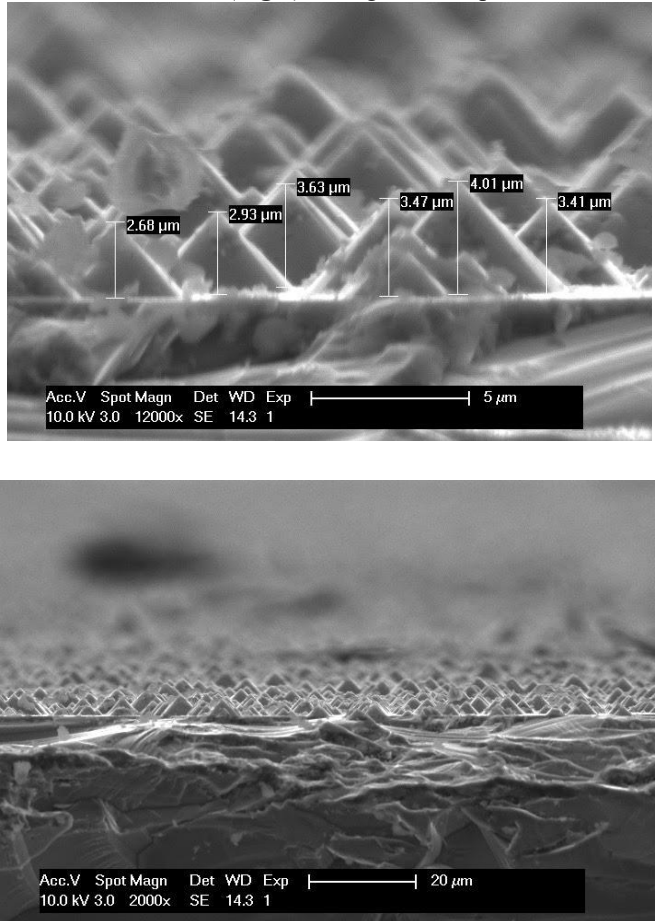


**Fig. 5.** The pyramidal structures that have formed as a result of the chemical etching process. The base angle is fixed due to the process, and results in a semi-random distribution of pyramidal structured silicon of nominally sized between 2.5 and 5 µm

pyramids depend on the concentration of the etching solution and the etching time, as can be observed in Fig.5. Further, an extra MACE step is used so the structures become hierarchically textured, as can be observed in Fig. 7. To form the nanowires on the pyramids' walls, the wafer with the pyramid structures is submerged in an aqueous solution at room temperature containing 5M HF and 20 mM Ag. We tested the etching time from 1 to 5 minutes, which increased the etched area and nanowire length up to 0.8 µm. This additional step is performed to further decrease the structure's reflectivity and has been shown to be effective at reducing the surface average reflectivity [4-6]. Additionally, it has been shown that the hierarchical structuring improves the hydrophobic properties of the black silicon [5]. Further processing with a chemical coating would improve this property to make it superhydrophobic – making it extremely attractive for applications where self-cleaning or fluid corrosion/exposure resistance is preferred.

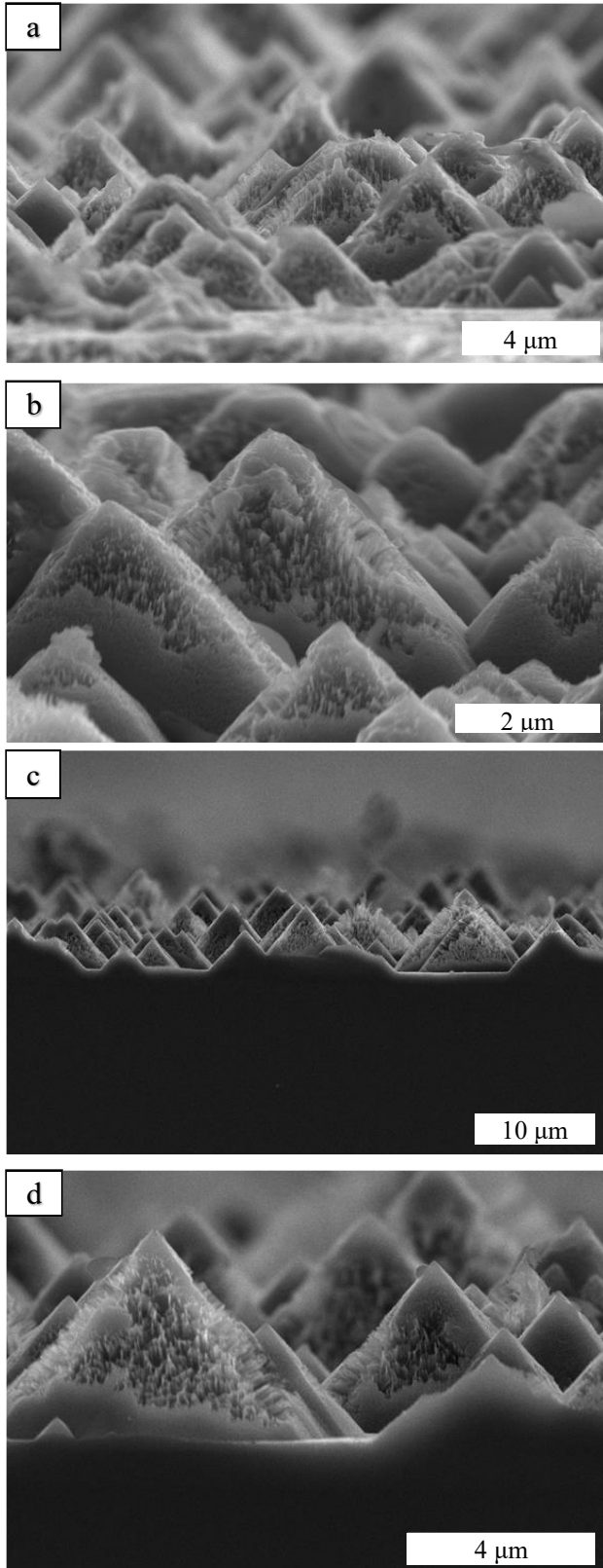


**Fig. 6 (a,b):** Sample etched with a metallic etchant for 4 minutes, **(c,d)** Sample etched for 5 minutes. The sample etched for 5 minutes highlights much stronger peaks and nanowire-like hierarchical structuring at the surface.

### Experimental Characterization

Once fabricated, the optical properties of black silicon are characterized by absorption and reflection spectroscopy using a commercial spectrometer Jasco V-670 UV-Vis Photospectrometer with a 60 mm integrating sphere within the wavelength region of 500 nm to 2.5  $\mu\text{m}$  (UV-Vis-NIR), and by Fourier-Transform Infrared Spectroscopy (FTIR) for wavelengths between 2.5  $\mu\text{m}$  and 20  $\mu\text{m}$  (mid-IR). The Jasco V-670 optical system offers automatically exchanged dual-grating and dual detector capabilities, and a unique single monochromator design that utilizes fewer mirrors, providing higher throughput, which results in a higher signal-to-noise ratio for the entire spectral range of 190 nm and 2700 nm. For these measurements, however, we eliminate potential errors at the extreme wavelengths and choose to measure between 500-2500 nm. All measurements in UV-Vis spectrometer are calibrated against a standard Teflon white body, and the reflectivity spectrum was compared with theoretical models, validating the experimental capabilities of the optical system. As the UV-Vis instrumentation is limited to the near infrared range, a Fourier-Transform Infrared Spectroscopy (FTIR) setup is used to verify the emissivity spectra in the mid-infrared range. Utilizing a diamond ATR probe, emissivity comes as an indirect measurement assuming that the structure is opaque and the transmissivity (native measurement to the process) can be transformed mathematically into reflectivity. The results of the two measurements (Fig. 7) demonstrate a highly anti-reflective surface, and a high degree of alignment with the predicted values for reflectivity. There is a deviation with the predictions between the optical/NIR wavelengths (500-2200 nm) as measured by the UV-Vis photospectrometer. The discrepancy is likely due to the sample not completely filling the integrating sphere's measurement area; further work will produce larger samples that will eliminate any errors that might occur from measuring only a partially covered measurement surface area (integrating sphere aperture).

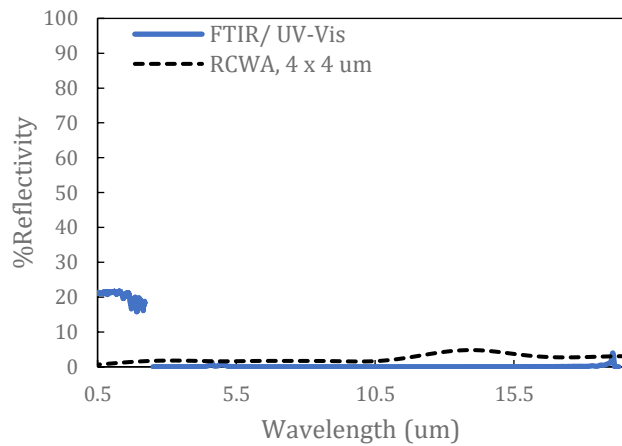


**Fig.7.** Experimentally measured values for reflectivity of the sample shown in Fig. 6 (c,d) compared with predicted values measured in RCWA for a 5  $\mu\text{m}$  x 5  $\mu\text{m}$  micropyramid. As expected, the reflectivity in the IR-region (as measured by an FTIR device) is below 3%, with an average value of approximately 1.5%.

## CONCLUSION

Black Silicon is well-studied as an anti-reflective coating, but past literature has often focused on producing high-quality nearly perfectly anti-reflective coatings for optical, solar, and instrumentation applications. Here we demonstrate that a relatively inexpensive mechanical etching process, that requires minimal setup and equipment, can be used to create surfaces that are still highly anti-reflective. Further, we demonstrate that the reduced reflection continues into the IR-spectrum, with a reflectivity that remains minimal through the heat-transfer relevant IR-wavelength region of 9-13 um. Under minimal solar incidence and when exposed to the atmosphere, the surface temperature is predicted to be 3.6° C beneath the ambient value, compared to the 4.2° C temperature increase (relative to ambient) predicted for bare silicon. The 8°C delta corresponds to an approximated 180 W/m<sup>2</sup> cooling power increase over bare silicon (at a surface temperature of 50° C), meaning the microstructuring results in significantly higher cooling relative to bare silicon. This is in addition to the surface becoming hydrophobic. Thus, this material becomes attractive for a variety of cooling applications as it is not able only to cool more efficiently than traditional metals and semi-metals, it can also self-clean –all completely passively and without the need for power input.

## REFERENCES

- [1] Oh Jihun, Hao-Chih Yuan, Howard M. Branz, An 18.2%-efficient black-silicon solar cell achieved through control of carrier recombination in nanostructures, *Nat. Nanotechnol.* 7 (2012) 743–748.
- [2] G. Barillaro, A. Nannini, M. Piotto, Electrochemical etching in HF solution for silicon micromachining, *Sens. Actuators, A* 102 (2012) 195–201.
- [3] M.P. Stewart, J. Buriak, Chemical and biological applications of porous silicon technology, *Adv. Mater.* 12 (2000) 859–869.
- [4] Y. Huang, W. Yan, X. Tan, and L. He, “Study on silicon nanopillars with ultralow broadband reflectivity via maskless reactive ion etching at room temperature,” *Mater. Sci. Eng. B Solid-State Mater. Adv. Technol.*, vol. 223, pp. 153–158, 2017.
- [5] Y. Liu, A. Das, Z. Lin, I. B. Cooper, A. Rohatgi, and C. P. Wong, “Hierarchical robust textured structures for large scale self-cleaning black silicon solar cells,” *Nano Energy*, vol. 3, pp. 127–133, 2014.
- [6] Wensheng Yan, Stephan Dottermusch, Christian Reitz, Bryce S. Richards, Hexagonal arrays of round-head silicon nanopillars for surface anti-reflection applications, *Appl. Phys. Lett.* 109 (2016). 143901–1–143901–5.
- [7] Yi Huang, Wu Wei Wang, Weizhong Chen Pan, Zhen Wang, Xinyu Tan, Wensheng Yan, Comparative investigation on designs of light absorption enhancement of ultrathin crystalline silicon for photovoltaic applications, *J. Photonics Energy* 6 (4) (2016). 047001-1–047001-10.
- [8] X. Liu, P.R. Coxon, M. Peters, B. Hoex, J.M. Cole, D.J. Fray, Black silicon: fabrication methods, properties and solar energy applications, *Energy Environ. Sci.* 7 (2014) 3223–3263.
- [9] Jing Yang, Fangfang Luo, Tsung Sheng Kao, Xiong Li, Ghim Wei Ho, Jinghua Teng, Xiangang Luo, Minghui Hong, Design and fabrication of broadband ultralow reflectivity black Si surfaces by laser micro/nanoprocessing, *Light: Sci. Appl.* 3 (2014). e185-1–e185-8.
- [10] Hao-Chih Yuan, Vernon E. Yost, Matthew R. Page, Paul Stradins, Daniel L. Meier, Howard M. Branz, Efficient black silicon solar cell with a density-graded nanoporous surface: optical properties, performance limitations, and design rules, *Appl. Phys. Lett.* 95 (2009). 123501-1–123501-3.
- [11] Zhipeng Huang, Nadine Geyer, Peter Werner, Johannes de Boor, Ulrich Gösele, Metal-assisted chemical etching of silicon: a review, *Adv. Mater.* 23 (2011) 285–308.
- [12] L.L. Ma, Y.C. Zhou, N. Jiang, X. Lu, J. Shao, W. Lu, J. Ge, X.M. Ding, X.Y. Hou, Wide-band “black silicon” based on porous silicon, *Appl. Phys. Lett.* 88 (2006). 171907-1–171907-3.
- [13] H.M. Shang, Y. Wang, K. Takahashi, G.Z. Cao, D. Li, Y.N. Xia, *J. Mater. Sci.* 40 (2005) 3587–3591.
- [14] Y. Liu, Z.Y. Lin, W. Lin, K.S. Moon, C.P. Wong, *ACSAppl. Mater. Interfaces* 4 (2012) 3959–3964.
- [15] Y. Liu, W. Lin, Z. Y. Lin, Y. H. Xiu, C. P. Wong, *Nanotechnology*, 23 (2012) 255703.
- [16] M. A. Green. Self-consistent optical parameters of intrinsic silicon at 300K including temperature coefficients, *Sol. Energ. Mat. Sol. Cells* 92, 1305–1310 (2008)
- [17] C. D. Salzberg and J. J. Villa. Infrared Refractive Indexes of Silicon, Germanium and Modified Selenium Glass, *J. Opt. Soc. Am.*, 47, 244-246 (1957)
- [18] B. Tatian. Fitting refractive-index data with the Sellmeier dispersion formula, *Appl. Opt.* 23, 4477-4485 (1984)
- [19] Michael H. Jones, Stephen H. Jones. Optical Properties of Silicon. *Virginia Semi-Conductor, Inc.* [http://www.univie.ac.at/photovoltaik/vorlesung/ss2014/unit4/optical\\_properties\\_silicon.pdf](http://www.univie.ac.at/photovoltaik/vorlesung/ss2014/unit4/optical_properties_silicon.pdf)
- [20] Reflectivity of Aluminium- UV, Visible and Infrared. *Laser Beam Products – Precision Optics*. <https://laserbeamproducts.wordpress.com/2014/06/19/reflectivity-of-aluminium-uv-visible-and-infrared/>